Biosensors and Bioelectronics 219 (2023) 114818

Contents lists available at ScienceDirect

Biosensors and Bioelectronics

journal homepage: www.elsevier.com/locate/bios

Directed evolution of diacetylchitobiose deacetylase via high-throughput droplet sorting with a novel, bacteria-based biosensor

Guoyun Sun [a,b], Yaokang Wu [a,b], Ziyang Huang [b], Yanfeng Liu [a,b], Jianghua Li [b], Guocheng Du [a,b], Xueqin Lv [a,b], Long Liu [a,b,*]

[a] Key Laboratory of Carbohydrate Chemistry and Biotechnology, Ministry of Education, Jiangnan University, Wuxi, 214122, China
[b] Science Center for Future Foods, Jiangnan University, Wuxi, 214122, China

ARTICLE INFO

Keywords:
Droplet sorting
Biosensor
Directed evolution
Diacetylchitobiose deacetylase

ABSTRACT

Numerous biological disciplines rely on high-throughput cell sorting. Flow cytometry, the current gold standard, is capable of ultrahigh–throughput cell sorting, but measurements are primarily limited to cell size and surface marker. Droplet sorting technology is gaining increasing attention with the ability to provide an individual environment for the analysis of single-cell secretion. Although various droplet detecting methods, such as fluorescence, absorbance, mass spectrum, imaging analysis, have been developed for droplet sorting, it remains challenging to establish high-throughput sorting methods for numerous analytes. We aim to develop a high-throughput sorting system based on the glucosamine (GlcN) measurement for the directed evolution of diacetylchitobiose deacetylase (Dac), the key enzyme for GlcN production. To overcome the limitation that no high-throughput sorting system existed for GlcN, we designed a novel bacteria-based biosensor capable of converting GlcN to a positively correlated fluorescence signal. Through characterization and optimization, it was possible to detect GlcN in droplets for high-throughput droplet sorting. We recovered the best Dac mutant S60I/R157T/F168S after sorting ~0.2 million Dac mutants; its activity was 48.6 ± 1.5 U/mL, which was 1.8-times that of our previously discovered Dac mutant R157T (27.2 ± 1.8 U/mL). This result successfully demonstrated the combination of high-throughput droplet sorting technology and a bacteria-based biosensor, which could facilitate the industrial production of GlcN and serve as a model for similar droplet sorting applications.

1. Introduction

Sorting cells of interest are fundamental to synthetic biology, clinical research, drug discovery, and other fields (Gach et al., 2017; Heath et al., 2016; Liu et al., 2022; Sivaramakrishnan et al., 2020; Sun et al., 2020; Tavakoli et al., 2019). Currently, the most effective cell sorting technology is commercial flow cytometry, which enables ultrahigh throughput cell sorting (Doan et al., 2018; Lance et al., 2016; Lim and Abate, 2013). However, since all cells share the same environment, this restricts its analysis of cell secretion. This limitation can be circumvented with droplet microfluidics, which can provide a chemical barrier between cells (Joensson and Andersson Svahn, 2012; Wen et al., 2016). In the past decade, numerous droplet sorting platforms with enhanced throughput and accuracy have been developed (Isozaki et al., 2020; Schutz et al., 2019; Xi et al., 2017).

The key step in performing droplet sorting is generating detectable signals in droplets. Various droplet sorting measuring techniques, including fluorescence, absorbance, mass spectrum, and imaging analysis, have been developed to date (Anagnostidis et al., 2020; Duncombe et al., 2021; Fu et al., 2021; Gielen et al., 2016; Holland-Moritz et al., 2020; Pan et al., 2019). Imaging analysis is typically used for cell density or morphology analysis among these techniques (Anagnostidis et al., 2020; Watterson et al., 2020). Although the mass spectrum can provide comprehensive information about a droplet's constituents, the droplet itself is lost during the analysis process (Smith et al., 2013; Wink et al., 2018). However, although droplet splitting is a possible solution, sorting throughput is still limited due to the time-consuming mass spectrum analysis and synchronization of split droplets (Holland-Moritz et al., 2020). Fluorescence remains the most prevalent droplet sorting signal. Since droplet washing is inapplicable, the Förster resonance energy transfer (FRET) sensor is one of the best droplet fluorescence sensors. With specific nucleic acid hybridization or enzyme cleavage, the FRET sensor's fluorophore and quencher are separated, releasing fluorescent signals (Hyman et al., 2021; Liu et al., 2020; Ng et al., 2019). FRET

* Corresponding author. Key Laboratory of Carbohydrate Chemistry and Biotechnology, Ministry of Education, Jiangnan University, Wuxi, 214122, China.
E-mail address: longliu@jiangnan.edu.cn (L. Liu).

https://doi.org/10.1016/j.bios.2022.114818
Received 23 August 2022; Received in revised form 2 October 2022; Accepted 12 October 2022
Available online 17 October 2022

sensors are typically designed for nucleic acids and specific enzymes. Generating fluorescent or colorful products is another popular method for droplet measurement, but it is not always possible to detect small molecules in droplets (Gielen et al., 2016; Qiao et al. 2017, 2022).

In our case, we are interested in determining the concentration of glucosamine (GlcN) in droplets to realize the activity improvement of diacetylchitobiose deacetylase (Dac) through directed evolution. As a fundamental component of cartilage tissue, GlcN is regarded as an essential supplement for osteoarthritis patients (Bruyere et al., 2016; Nakamura, 2011). The commercial production of GlcN is based on the hydrolysis of chitin or chitosan from crab and shrimp shells, which involves the use of strong acid and may trigger allergic reactions in some individuals (Liu et al., 2013; Sitanggang et al., 2010). Due to the mild conditions and environmental friendliness, the Dac-catalyzed production of GlcN from N-acetylglucosamine (GlcNAc) is gaining popularity (Jiang et al. 2018, 2019). Although numerous attempts have increased the activity and expression of Dac, additional progress is necessary to increase the economic advantage of enzymatic GlcN production (Huang et al., 2021; Mao et al., 2021). Notably, previous studies have determined that directed evolution is a promising method for enhancing Dac activity (Gach et al., 2017). By generating numerous Dac mutants and selecting the most effective, it is possible to obtain Dac with enhanced catalytic efficiency. However, while high-throughput sorting of positive Dac mutants is required for this strategy, no relevant method has been established for GlcN or Dac.

In this work, a high-throughput droplet sorting system with a bacteria-based biosensor is proposed for the directed evolution of Dac (Fig. 1). Firstly, random mutations of the Dac gene were generated using error-prone polymerase chain reaction (epPCR) and expressed by *Bacillus subtilis*. After transformation, a single bacterium was encapsulated within a droplet and incubated for 24 h to allow Dac expression and accumulation. The GN1 bacteria were injected into the incubated droplets with the substrate GlcNAc. The Dac catalytic product GlcN induced the expression of enhanced green fluorescent protein (eGFP) in the GN1 strain. After the second 24 h of incubation to allow the expression of eGFP, droplets could be sorted using a high-throughput droplet sorter. Following 3 h of high-throughput droplet sorting, we screened ~0.2 million mutants and recovered strain M7 as the best. With the S60I/R157T/F168S mutation, the activity of this Dac mutant increased to 48.6 ± 1.5 U/mL, which was 1.8 times that of our previously discovered Dac mutant R157T (27.2 ± 1.8 U/mL) (Jiang et al., 2019). Additionally, the kinetic constants of this Dac mutant were enhanced. This work was the first to demonstrate high-throughput droplet sorting based on GlcN measurement; the strategy could also be extended to similar applications.

2. Material and methods

2.1. Strain preparation and mutant library construction

The recombinant plasmid pP43NMK for Dac expression was obtained from our previous work (Mao et al., 2021). The mutant Dac genes were generated using epPCR (QuickMutation, Beyotime Biotechnology, China) and cloned using the Seamless Cloning Kit into the plasmid pP43NMK (Beyotime Biotechnology, China). *Escherichia coli* JM109 was utilized for the construction and duplication of plasmids, whereas *Bacillus subtilis* WB600 was the expression host for Dac. 12 h were spent cultivating all strain seeds in 2 mL Luria-Bertani (LB) medium at 37 °C with 220 rpm shaking. For the measurement of Dac activity, 1 mL of *B. subtilis* seed cultures were added to a 50 mL Terrific broth (TB) medium at 37 °C and shaken at 220 rpm for 72 h. If necessary, appropriate antibiotics (100 μg/mL ampicillin, 10 μg/mL for kanamycin, chloromycetin, 5 μg/mL) were administered.

The GlcN-detecting strain GN1 was constructed as follows. First, the GlcN transporter encoded by *gamP* was restored in a previously constructed *B. subtills* strain BNY0 (*B. subtilis* 168 △*nagP*△*gamP*△*gamA*△*ldh*△*pta*△*glcK*△*pckA*△*pyk*△*gamR*:lox72, △*nagAB*:P_{veg}-*yqaB*, P_{veg}-*glmS*) to generate strain BNYP, which lack the main catabolic pathway of GlcN6P and thereby can accumulate GlcN6P in the cells by assimilating GlcN (Wu et al., 2020). Then, the genetic cassette containing eGFP under the control of the GlcN6P-responsive promoter P_{sg2} was constructed. In order to reduce the leaky expression of eGFP, the repressor LacI and corresponding operator LacO were added to the genetic cassette. Eventually, the eGFP expression cassette was integrated into the *aprE* locus of BNYP, producing strain GN1.

All the primer synthesis and DNA sequencing were performed by Genewiz (Suzhou, China).

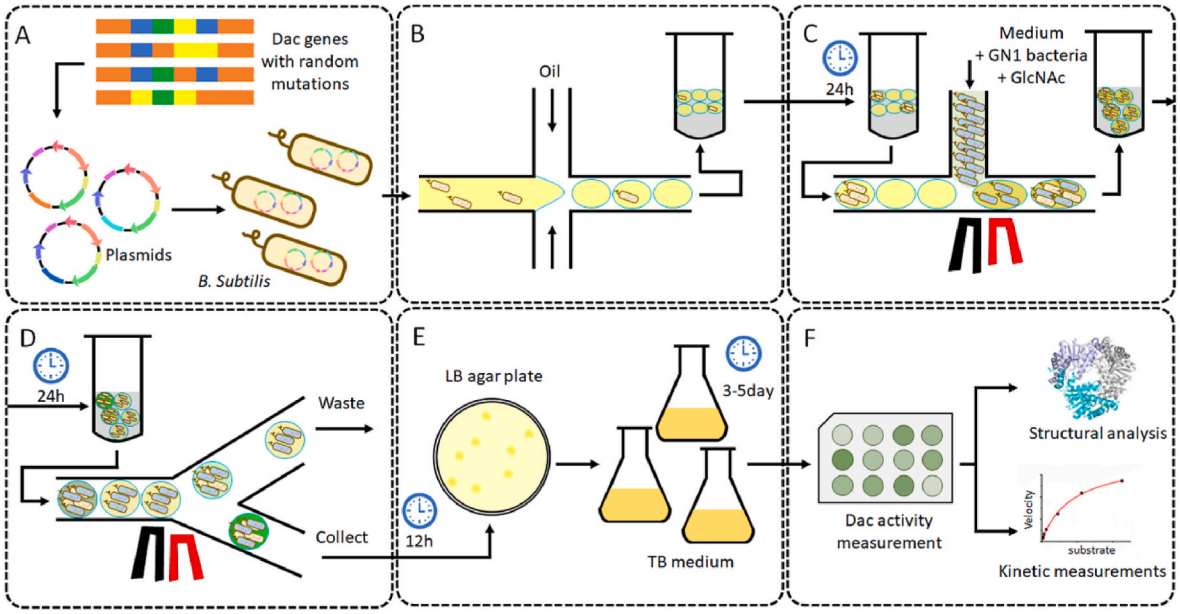

Fig. 1. Schematic illustrating high-throughput droplet sorting for directed evolution of Dac using a bacteria**-based biosensor.** (A) Construction of a Dac mutant library. (B) Single bacterium encapsulation and culture in a droplet. (C) Droplet injection with substrate and GN1 bacteria. (D) High-throughput droplet sorting. (E) Positive bacteria recovery and fermentation. (F) Characterization of positive Dac mutant.

2.2. Measurement of dac activity

The activity of Dac was determined using the deacetylation of GlcNAc. After 72 h of culturing of Dac-expressing bacteria, the fermentation broth was centrifuged at 12,000×*g* for 2 min, 200 μL of the supernatant was collected, and was mixed with 200 μL 100 g/L GlcNAc solution (dissolved 50 mM PB, pH = 8.0), which was prewarmed at 40 °C. Then, the solution was incubated at 40 °C and shaken at 1000 rpm for 2 min; 10 μL of solution was immediately collected and added to 190 μL of PB solution (pH = 8.0). After 10 s of mixing at 1000 rpm, 5 μL solution was added to 100 μL *o*-Phthalaldehyde (OPA), detecting the reagent after 10 s of mixing at 1000 rpm. The OPA reagent consisted of a 100 mM sodium carbonate buffer (pH = 10.5) with 500 mg/L OPA, 1% (v/v) ethanol, and 1 mM dithiothreitol added to it. The absorbance at 330 nm was determined after the solution was shaken at 1000 rpm using a spectrophotometer (Thermo Scientific, Vantaa, Finland). The same procedure was followed for the blank reference, except the GlcNAc concentration was 0 g/L. The absorbance difference was calculated and compared with the stand GlcN curve to determine the concentration of produced GlcN. One Dac activity unit corresponds to the production of 1 μmol GlcN in 1 min. Unless otherwise specified, all chemicals were purchased from Sangon Biotech (Shanghai, China).

2.3. Fabrication of microfluidic devices

Microfluidic devices included in this work were a droplet generator, droplet injector, droplet sorter, and observing chamber, in accordance with previous designs (Guo et al., 2018; Liu et al., 2020; Mazutis et al., 2013; Ng et al., 2015). Briefly, microfluidic devices were fabricated using polydimethylsiloxane (PDMS, Sylgard 184, Dow Corning Inc., Midland, MI) and bonded by plasma (Baraket et al. 2013, 2016, 2017; Lee et al., 2015). The detail of microfluidic device fabrication was introduced in Supporting Information (SI) Supplementary 1.

2.4. Single bacteria encapsulation

After transformation with the Dac mutant plasmid, *B. subtilis* was cultured in an LB medium containing kanamycin for 6 h. The bacteria were then rinsed with fresh TB medium and diluted to OD_{600} of 0.05 (the concentration of *B. subtilis* was 5×10^6/mL). Since the cell distribution in droplets followed Poisson statistics, 10% of droplets (diameter was ~30 μm) contained a single bacterium, less than 0.5% contained more than one bacterium, and the remaining droplets were empty. The bacteria solution was collected in a 1 mL syringe; the oil phase was HFE 7500 (3M, USA) containing 2% (v/v) Pico-Surf surfactant (5% in HFE 7500, Sphere Fluidics). The connection between the syringe and the microfluidic device was made using polyethylene tubing with an inner diameter of 0.38 mm and an outer diameter of 1.03 mm. The syringes were driven by syringe pumps (PHD2000, Harvard, USA), with flow rates of 10 μL/min and 4 μL/min for spacing oil and bacteria solution, respectively. Before injection, the generated droplets were incubated at 37 °C with 220 rpm shaking for 24 h in an inverted syringe.

2.5. Droplet injection of GlcN detecting bacteria

In order to measure the secreted Dac activity in droplets, GN1 bacteria, GlcNAc, and isopropyl-β-D-thiogalactoside (IPTG) were incorporated into the injecting solution. First, the GlcN-detecting strain GN1 was grown in a TB medium for 12 h. The GN1 bacteria were then washed with fresh TB medium, and the concentration was adjusted to OD_{600} was 11.1. Next, 10% (v/v) GlcNAc solution (100 g/L, pH = 8.0) and 0.2% (v/v) IPTG (1.0 M) were added to the syringe-collected bacteria solution. Consequently, the final cell density for GN1 in the injecting solution was OD_{600} of 10.0; the final concentration of GlcNAc was 10 g/L, and the final concentration of IPTG was 2.0 mM (2x). To maintain the suspension of GN1 bacteria, a small, sterile magnetic stirrer bar was inserted into the syringe and driven by a neodymium magnet. Another syringe was used to collect the droplets containing Dac-expressing bacteria that had been incubated. Flow rates were set to 8 μL/min, 0.8 μL/min, and 1 μL/min for the oil phase, detecting bacteria, and incubating Dac-expressing bacteria. To realize droplet injection, Arduino UNO generated an electric signal with 2 V amplitude and 10 kHz frequency, which was then amplified to 100V by an amplifier (PinTech, Shenzhen). Before sorting, the injected droplets were also collected in an inverted-placed syringe and incubated at 37 °C with 220 rpm shaking for 24 h before sorting.

2.6. Droplet sorting and recovering of positive mutants

With a flow rate of 0.5 μL/min, the incubated droplets were injected into the droplet sorter, resulting in a throughput of 200 droplets/s. The spacing oil flow rate was 15 μL/min. The droplet's fluorescence was excited by white LED light with the corresponding filters (Ex/Em: 495/525 nm) in an inverted microscope (DMi-8, Leica); the emission fluorescent light was detected by a photomultiplier tube (PMT; H10721, Hamamatsu) and analyzed by Arduino DUE. Once the fluorescent signal of a droplet exceeded the threshold, Arduino UNO generated an electric signal with 5 V amplitude, 10 kHz frequency, and 4 ms duration, which was amplified to 800 V by an amplifier. After droplet sorting, the collected droplets were placed in a 1.5 mL tube containing 100 μL demulsifier 1H,1H,2H,2H-perfluoro-1-octanol (Aladdin), and 100 μL LB medium. Mixing the solution and transferring the aqueous phase (collected cells) to an LB agar plate containing kanamycin allowed only Dac-expressing bacteria to grow on the plate (GN1 only resisted chloromycetin). After 12 h of growth at 37 °C, single colonies were isolated and cultured in TB to measure enzyme activity.

3. Results and discussion

3.1. Characterization of GlcN detection by GN1

To enable the measurement of Dac activity in droplets, we engineered the strain GN1 capable of converting GlcN, the product of Dac catalysis, into a fluorescent signal for droplet measurement. Strain GN1 could utilize GlcN to produce glucosamine-6-phosphate (GlcN6P), which then triggers the synthesis of eGFP when coupled with IPTG; a high concentration of GlcN6P could speed up the eGFP synthesis and result in a stronger fluorescence. Meanwhile, *nagP*, which encodes the GlcNAc transporter protein, was deleted from GN1. Therefore, GN1's eGFP expression is only related to GlcN and is unaffected by the substrate GlcNAc.

First, the GN1 response was measured on a milliliter scale for standard GlcN: 1 mL of GN1 cultured for 24 h was combined with 1 mL of fresh TB medium containing 2.0 mM IPTG (2x IPTG) and various concentrations of GlcN, ranging from 0 to 10 g/L. After mixing, the concentration for IPTG was 1.0 mM (1x), and concentrations for GlcN ranged from 0 g/L to 5 g/L (similar calculations were omitted below). Moreover, a final concentration of 5 g/L GlcNAc was added to the GN1 solution to confirm that the substrate GlcNAc would not induce fluorescence in GN1. After 24 h of incubation, the fluorescence was measured using a spectrophotometer (Ex/Em: 495/525 nm, same as below), and the results are depicted in Fig. 2A. We found that eGFP expressed by GN1 bacteria was positively correlated to GlcN in the range of 0–1.5 g/L, which was determined by the intrinsic properties of the transcriptional factor GamR, and this range was consistent with that (0–10 mM) observed in our previous study (Wu et al., 2020). Meanwhile, GlcNAc (with and without GlcN) did not influence GlcN measurement. The preceding experiment demonstrated that GN1 could act as a GlcN sensor to measure GlcN concentration.

The next step involved optimizing the substrate GlcNAc concentration. Here, we constructed the strains M1 and M2, which expressed the wildtype Dac and R157T Dac mutant, respectively, as the Dac-

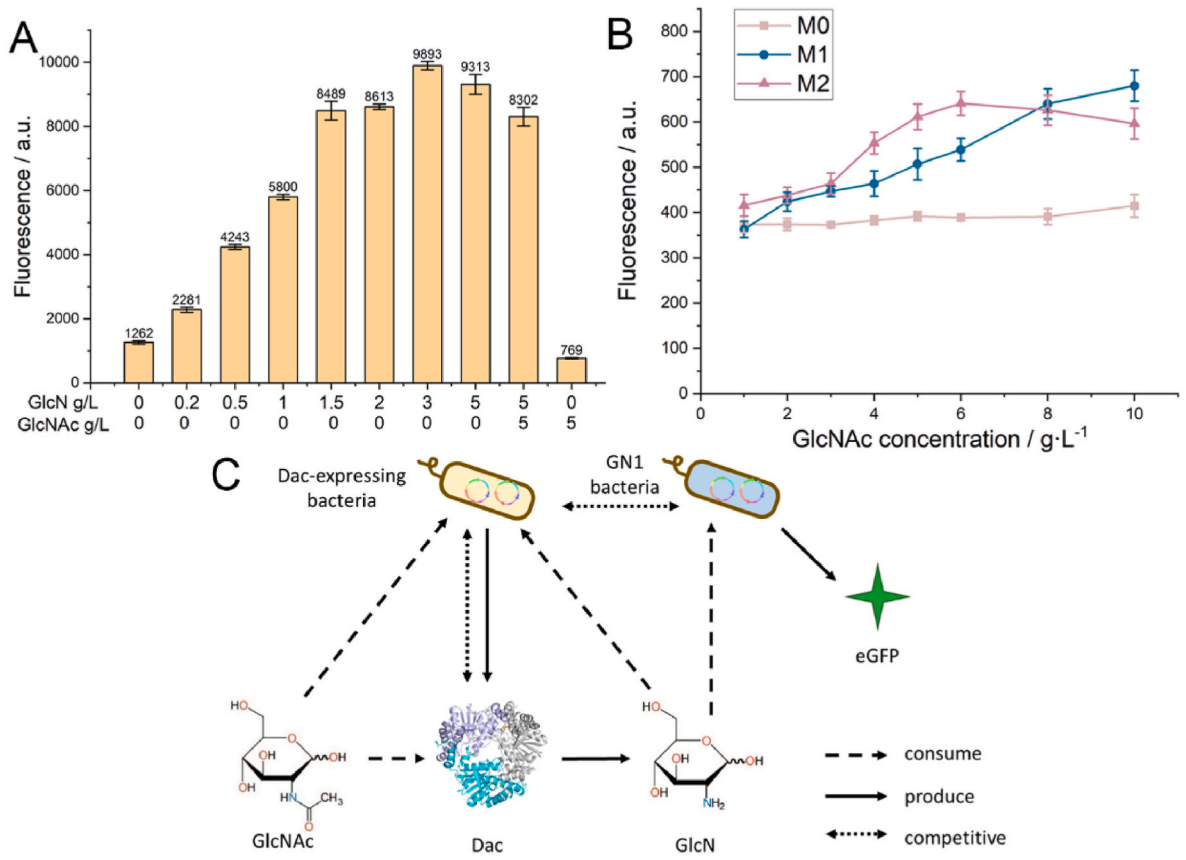

Fig. 2. Characterization of GN1 response and eGFP production schematic. (A) GN1 response against different GlcN concentrations with and without GlcNAc. (B) GN1 response against different GlcNAc concentrations and Dac-expressing strains. (C) Schematic figure of the competitive utilization of GlcNAc and GlcN in the production of eGFP.

expressing strains for characterization. In a previous study, we discovered the Dac mutant R157T, which was more active than the wildtype (Jiang et al., 2019). We also constructed the strain M0, whose plasmid lacked the Dac gene for characterization. Similar to the droplet experiment, 1 mL of GN1 bacteria were washed with fresh TB medium containing 2x IPTG and 2x GlcNAc in concentrations ranging from 2 to 20 g/L. Then, 1 mL GN1 solution was mixed with 1 mL Dac-expressing strains, which were already cultured for 24 h; the mixed solution was cultured for another 24 h before fluorescent measurement. As depicted in Fig. 2B, the optimal concentration of GlcNAc (after a 1:1 dilution) was 5 g/L, demonstrating a greater difference between strains M1 and M2. Although higher concentration of GlcNAc could induce higher fluorescence, the difference between M1 and M2 was actually decreased. Meanwhile, high concentration of GlcNAc (GlcN) might induce lower fluorescence of GN1, since accumulation of GlcNAc was toxic for GN1 (Wu et al., 2020). Therefore, moderate concentration of GlcNAc was more suitable for Dac activity measurement.

In fact, the substrate GlcNAc was consumed by both enzyme Dac and Dac-expressing bacteria in the bacteria mixing solution (SI Supplementary 2), and the Dac-converted GlcN was also consumed by both Dac-expressing bacteria and GN1 bacteria (Fig. 2C). Therefore, if the expressed Dac showed higher activity, more GlcNAc could be converted to GlcN. Then, GN1 bacteria could utilize more GlcN, resulting in greater fluorescence.

3.2. Characterization of GlcN detection by GN1 in droplet

Similar characterization experiments were also conducted with droplets. First, fresh TB containing GlcN at concentrations ranging from 0 to 3 g/L was prepared and encapsulated separately into droplets. Then, GN1 bacteria with an OD_{600} of 10.0 and 2x IPTG were injected into these droplets. Therefore, after droplet injection, the concentration of GlcN was ranged from 0 to 1.5 g/L, where the induced fluorescence in GN1 was positively correlated (Fig. 2A). Here, the concentration of GN1 bacteria was identical to that of Dac-expressing bacteria after droplet incubation for 24 h (SI Supplementary 3). Therefore, in the droplet sorting experiment, the ratio of Dac-expressing bacteria to GN1 bacteria was intended to be 1:1. The injecting strategy demonstrated three benefits. Firstly, incubation allows Dac-expressing bacteria to accumulate sufficient Dac molecules to catalyze GlcNAc. Secondly, since both Dac-expressing bacteria and GN1 bacteria could utilize GlcN, injecting a similar number of GN1 bacteria could maintain comparable strength between Dac-expressing bacteria and GN1 bacteria. Thirdly, injecting multiple bacteria (GN1 bacteria) into droplets containing multiple bacteria (Dac-expressing bacteria) showed higher efficiency than single bacterium injection. In the current workflow, 10% droplets contained Dac-expressing bacteria before and after injection. However, compared with injecting single GN1 bacterium into the droplet containing single Dac-expressing bacterium, considering 10% single cell rate for both droplet encapsulation and injection operations, the success rate was only 1% (10% * 10%).

After 24 h of incubation, these droplets were injected into the observation chamber to capture fluorescent images. Fig. 3A displays the calculated and plotted average fluorescent intensities of various droplets. There was a positive correlation between fluorescent intensity and GlcN concentration. To validate Dac synthesis and catalysis in droplets, M0, M1, and M2 strains were encapsulated in droplets with single bacterium, incubated for 24 h, and injected with GN1 bacteria and GlcNAc. To further verify the optimal concentration of GlcNAc in droplets, different final concentrations of GlcNAc were tried. The

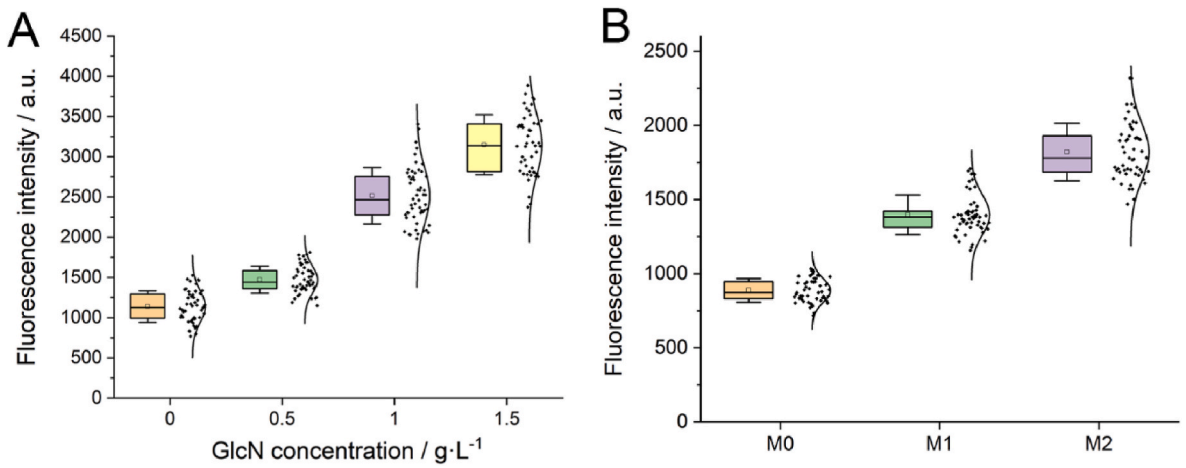

Fig. 3. Characterization of the GN1 response in droplets. (A) GN1 response to various GlcN concentrations in droplets. (B) GN1 response to various Dac-expressing strains with 5 g/L GlcNAc.

droplet results demonstrated that GlcNAc with the final concentration of 5 g/L was suitable for GlcN measurement (SI Supplementary 4). As illustrated in Fig. 3B, the fluorescent signals for strains M0, M1, and M2 were 886.9 ± 79.4, 1396.7 ± 133.0, and 1820.5 ± 192.9, respectively. These results demonstrated the accuracy of the proposed GlcN detection in droplets for distinguishing Dac with distinct activities. Therefore, the proposed GlcN biosensor and workflow were suitable for high-throughput droplet sorting of Dac mutants.

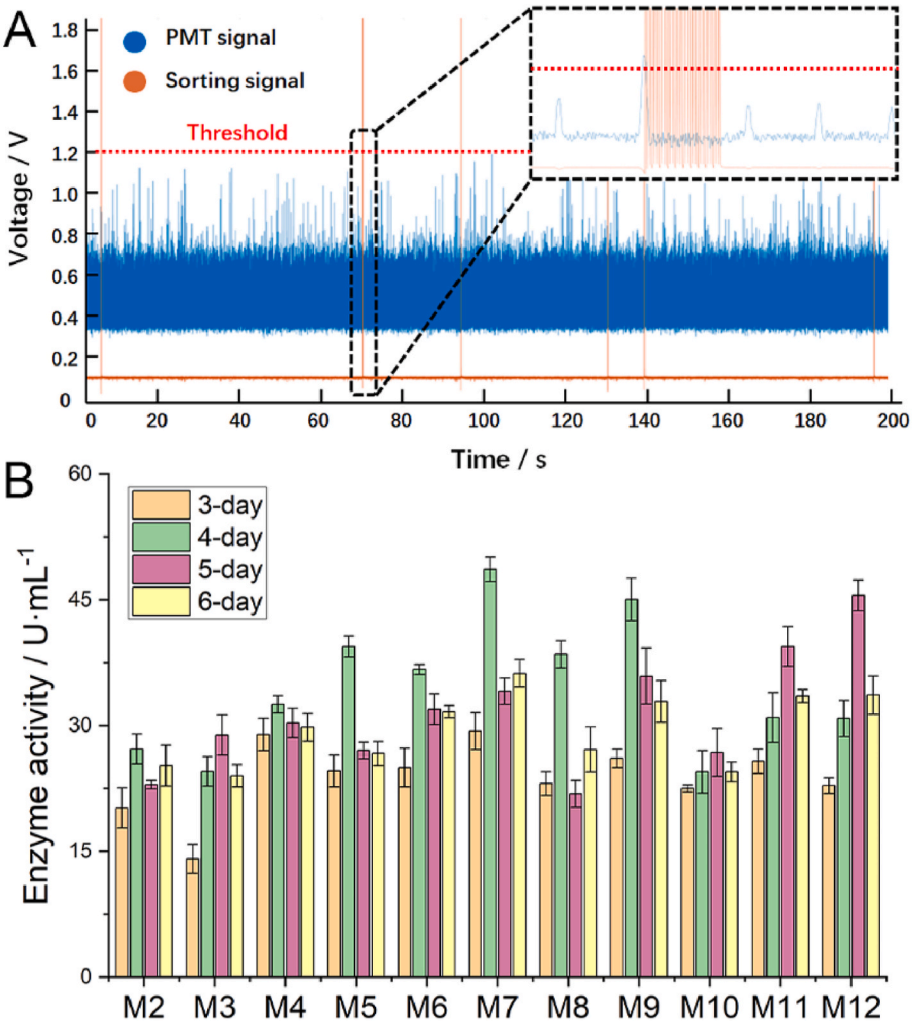

Fig. 4. Threshold setting and enzyme activity measurement. (A) Threshold setting for droplet sorting. (B) Enzyme activity of sorted mutants cultured for 3–6 days.

3.3. High-throughput droplet sorting for directed evolution of dac

The Dac mutant library was constructed using epPCR, with the positive Dac mutant R157T from our previous study serving as the template. As depicted in Fig. 1, single bacteria containing random Dac mutants were encapsulated in droplets, incubated, injected with GlcN detecting solution, and incubated again before droplet sorting. Then, the incubated droplets were re-injected into the droplet sorting device for high-throughput sorting. Droplet sorting procedure followed the standard protocol and was described in Section 2.6 (Mazutis et al., 2013). Based on the fluorescence readouts by PMT, high-throughput droplet sorting was performed with high accuracy (SI Supplementary 5). The threshold was set as the 0.1% highest signal of all droplets (Fig. 4A). Considering the single cell encapsulation rate was 10% when we generated droplets, 90% of droplets did not contain Dac-expressing bacteria. Therefore, this threshold was actually set to collect the top 1% Dac-expressing bacteria based on the Dac activity.

After 3 h of droplet sorting, ~2 million droplets were screened and sorted, while 10% of these droplets contained Dac-expressing bacteria. The sorted bacteria were extracted from the collected droplets and plated on LB agar for a 12-h culture. Individual colonies were isolated and inoculated into a TB medium for 3–6 days of fermentation. Among all mutants, many mutants (M3 to M12) exhibited higher Dac activities than M2, and the results were shown in Fig. 4B. Among these mutants, M7 had the highest activity (48.6 ± 1.5 U/mL) at 96 h of fermentation, which was 1.8 times that of M2 (27.2 ± 1.8 U/mL).

3.4. Characterization of improved dac mutants

Since strain M7 displayed the highest Dac activity among all positive mutants, the kinetic constants of strains M2 and M7 were measured to validate the positive mutation of Dac. The kinetic constants k_m and V_{max} of M2 and M7 were determined based on the nonlinear fitting of catalytic velocities against different concentrations of the substrate GlcNAc by collecting the supernatant of M2 and M7 culture solutions on Day 4. The GlcNAc concentrations ranged from 0.5 g/L to 50 g/L. As shown in Fig. 5A and B, V_{max} for strain M7 (755.9 ± 24.0 μM/s) was double that of strain M2 (368.8 ± 19.2 μM/s), which was consistent with the enhanced Dac activity of strain M7.

The mutant sites of the M7 strain were identified to analyze the underlying principle for enhanced enzyme activity using DNA sequencing. Compared to the strain M2 (R157T), M7 contained two additional mutant sites, S60I and F168S. According to the protein docking simulation, mutant S60I was far from the catalytic pocket of GlcNAc, whereas mutant F168S was close to the catalytic pocket (Fig. 5C and D); therefore, we hypothesized that mutant F168S was the primary contributor to Dac activity enhancement. Due to the presence of a phenyl group and the hydrophobic nature of F168, we hypothesized that the proximity between the phenyl group of F168 and the carboxyl group of GlcNAc prevented the entrance of substrate GlcNAc. By substituting hydrophilic S168 for hydrophobic F168, the phenyl group was converted to a hydroxymethyl group, which may facilitate the entrance and decomposition of GlcNAc.

4. Conclusion

In summary, a high-throughput droplet sorting system based on GlcN concentration was developed for the directed evolution of Dac, which could produce GlcN by catalyzing GlcNAc. A bacteria-based biosensor designed to convert GlcN to a fluorescent signal with a positive

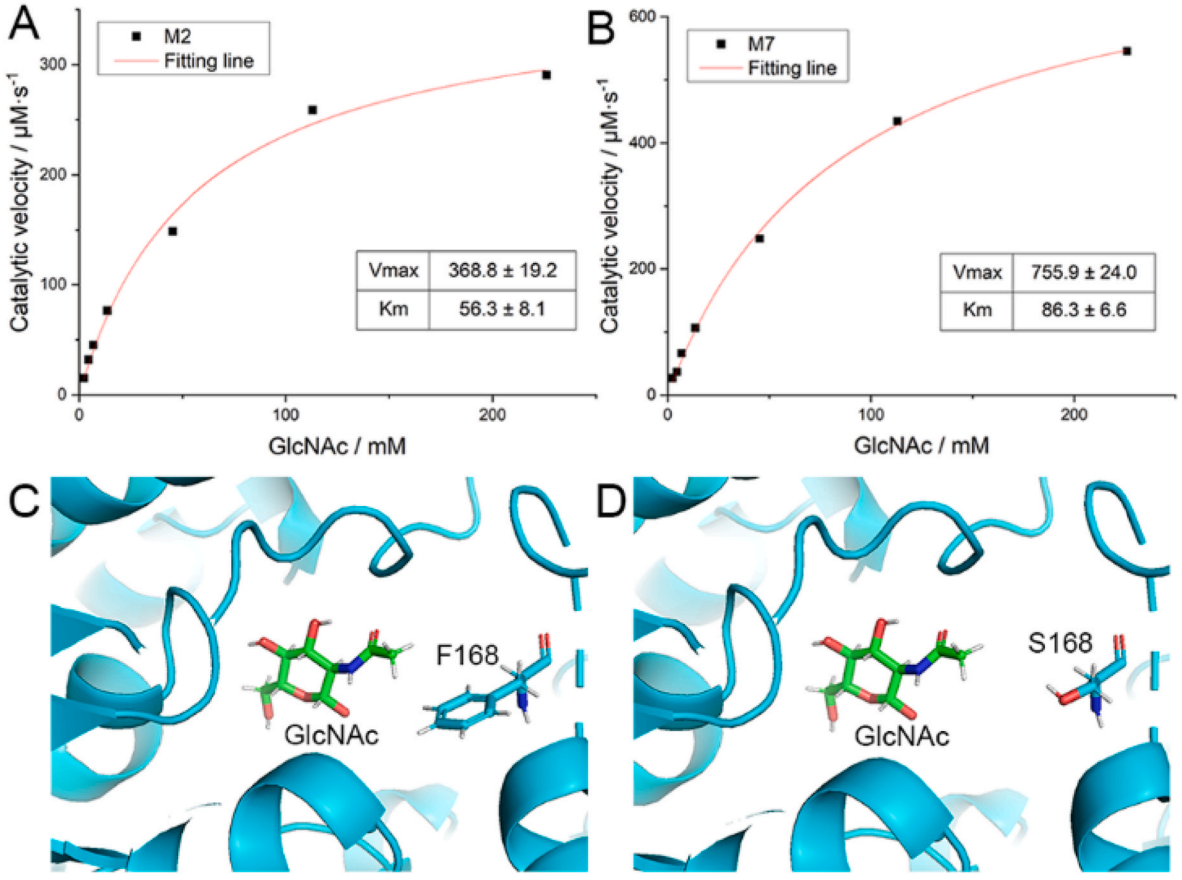

Fig. 5. Characterization of the positive mutant M7. (A–B) Nonlinear fitting for strain M2 (A) and M7 (B) kinetic constant measurements. (C–D) Docking of the strain M2 (C, R157T) and M7 (D, S60I/R157T/F168S).

correlation. Validation of GlcN detection by GN1 was conducted in both 96-well plates and droplets. Several mutants were recovered by generating random mutations of Dac and performing high-throughput droplet sorting, with the highest Dac activity reaching 48.6 ± 1.5 U/mL (M7), which was 1.8-times the original Dac mutant R157T (M2). Meanwhile, the V_{max} for M7 was also doubled compared to M2. These results successfully demonstrated high-throughput droplet sorting for the directed evolution of Dac, which is incredibly useful for promoting the industrial production of GlcN via environmentally friendly enzymatic catalysis. However, the current fluorescent response of GlcN via GN1 bacteria was not very accurate; many sorted Dac-expressing bacteria exhibited similar or slightly lower Dac activities compared with M2. The possible reasons could be cell heterogeneity between GN1 bacteria and droplet injection instability (the number of injected GN1 bacteria followed Poisson distribution).

Although the proposed biosensor and sorting system was demonstrated for GlcN measurement, it is straightforward to convert the measurements to other metabolic products by adapting the biosensor. In reality, designing a fluorescent reaction in a droplet to detect a specific product can be challenging due to the ultralow volume and limited operating methods of droplets. However, the system developed in this work demonstrated a successful combination of droplet microfluidics and a bacteria-based biosensor for high-throughput sorting. Moreover, the proposed system and its extension have broad applications in synthetic biology and other fields.

CRediT authorship contribution statement

Guoyun Sun: Conceptualization, Methodology, Investigation, Resources, Writing – original draft, Preparation. **Yaokang Wu:** Methodology. **Ziyang Huang:** Validation, Investigation. **Yanfeng Liu:** Supervision. **Jianghua Li:** Supervision. **Guocheng Du:** Project administration, Funding acquisition. **Xueqin Lv:** Conceptualization, Resources, Writing – review & editing, Project administration. **Long Liu:** Conceptualization, Writing – review & editing, Funding acquisition.

Declaration of competing interest

The authors declare that they have no known competing financial interests or personal relationships that could have appeared to influence the work reported in this paper.

Data availability

Data will be made available on request.

Acknowledgements

This work was financially supported by the National Natural Science Foundation of China (31930085, 32021005, 31870069), the Key Research and Development Program of China (2018YFA0900504, 2018YFA0900300), the Fundamental Research Funds for the Central Universities (JUSRP221013, JUSRP121010, JUSRP52019A).

Appendix A. Supplementary data

Supplementary data to this article can be found online at https://doi.org/10.1016/j.bios.2022.114818.

References

Anagnostidis, V., Sherlock, B., Metz, J., Mair, P., Hollfelder, F., Gielen, F., 2020. Deep learning guided image-based droplet sorting for on-demand selection and analysis of single cells and 3D cell cultures. Lab Chip 20 (5), 889–900.

Baraket, A., Lee, M., Zine, N., Sigaud, M., Bausells, J., Errachid, A., 2017. A fully integrated electrochemical biosensor platform fabrication process for cytokines detection. Biosens. Bioelectron. 93, 170–175.

Baraket, A., Lee, M., Zine, N., Yaakoubi, N., Bausells, J., Errachid, A., 2016. A flexible electrochemical micro lab-on-chip: application to the detection of interleukin-10. Microchim. Acta 183 (7), 2155–2162.

Baraket, A., Zine, N., Lee, M., Bausells, J., Jaffrezic-Renault, N., Bessueille, F., Yaakoubi, N., Errachid, A., 2013. Development of a flexible microfluidic system based on a simple and reproducible sealing process between polymers and poly (dimethylsiloxane). Microelectron. Eng. 111, 332–338.

Bruyere, O., Altman, R.D., Reginster, J.Y., 2016. Efficacy and safety of glucosamine sulfate in the management of osteoarthritis: evidence from real-life setting trials and surveys. Semin. Arthritis Rheum. 45 (4 Suppl. l), S12–S17.

Doan, M., Vorobjev, I., Rees, P., Filby, A., Wolkenhauer, O., Goldfeld, A.E., Lieberman, J., Barteneva, N., Carpenter, A.E., Hennig, H., 2018. Diagnostic potential of imaging flow cytometry. Trends Biotechnol. 36 (7), 649–652.

Duncombe, T.A., Ponti, A., Seebeck, F.P., Dittrich, P.S., 2021. UV-vis spectra-activated droplet sorting for label-free chemical identification and collection of droplets. Anal. Chem. 93 (38), 13008–13013.

Fu, X., Zhang, Y., Xu, Q., Sun, X., Meng, F., 2021. Recent advances on sorting methods of high-throughput droplet-based microfluidics in enzyme directed evolution. Front. Chem. 9, 666867.

Gach, P.C., Iwai, K., Kim, P.W., Hillson, N.J., Singh, A.K., 2017. Droplet microfluidics for synthetic biology. Lab Chip 17 (20), 3388–3400.

Gielen, F., Hours, R., Emond, S., Fischlechner, M., Schell, U., Hollfelder, F., 2016. Ultrahigh-throughput-directed enzyme evolution by absorbance-activated droplet sorting (AADS). Proc. Natl. Acad. Sci. U. S. A. 113 (47), E7383–E7389.

Guo, S., Lin, W.N., Hu, Y., Sun, G., Phan, D.T., Chen, C.H., 2018. Ultrahigh-throughput droplet microfluidic device for single-cell miRNA detection with isothermal amplification. Lab Chip 18 (13), 1914–1920.

Heath, J.R., Ribas, A., Mischel, P.S., 2016. Single-cell analysis tools for drug discovery and development. Nat. Rev. Drug Discov. 15 (3), 204–216.

Holland-Moritz, D.A., Wismer, M.K., Mann, B.F., Farasat, I., Devine, P., Guetschow, E.D., Mangion, I., Welch, C.J., Moore, J.C., Sun, S., Kennedy, R.T., 2020. Mass activated droplet sorting (MADS) enables high-throughput screening of enzymatic reactions at nanoliter scale. Angew Chem. Int. Ed. Engl. 59 (11), 4470–4477.

Huang, Z., Mao, X., Lv, X., Sun, G., Zhang, H., Lu, W., Liu, Y., Li, J., Du, G., Liu, L., 2021. Engineering diacetylchitobiose deacetylase from Pyrococcus horikoshii towards an efficient glucosamine production. Bioresour. Technol. 334, 125241.

Hyman, L.B., Christopher, C.R., Romero, P.A., 2021. Single-cell nucleic acid profiling in droplets (SNAPD) enables high-throughput analysis of heterogeneous cell populations. Nucleic Acids Res. 49 (18), e103.

Isozaki, A., Nakagawa, Y., Loo, M.H., Shibata, Y., Tanaka, N., Setyaningrum, D.L., Park, J.-W., Shirasaki, Y., Mikami, H., Huang, D., Tsoi, H., Riche, C.T., Ota, T., Miwa, H., Kanda, Y., Ito, T., Yamada, K., Iwata, O., Suzuki, K., Ohnuki, S., Ohya, Y., Kato, Y., Hasunuma, T., Matsusaka, S., Yamagishi, M., Yazawa, M., Uemura, S., Nagasawa, K., Watarai, H., Carlo, D.D., Goda, K., 2020. Sequentially addressable dielectrophoretic array for high-throughput sorting of large-volume biological compartments. Sci. Adv. 6 (22), eaba6712.

Jiang, Z., Lv, X., Liu, Y., Shin, H.D., Li, J., Du, G., Liu, L., 2018. Biocatalytic production of glucosamine from N-acetylglucosamine by diacetylchitobiose deacetylase. J. Microbiol. Biotechnol. 28 (11), 1850–1858.

Jiang, Z., Niu, T., Lv, X., Liu, Y., Li, J., Lu, W., Du, G., Chen, J., Liu, L., 2019. Secretory expression fine-tuning and directed evolution of diacetylchitobiose deacetylase by Bacillus subtilis. Appl. Environ. Microbiol. 85 (17).

Joensson, H.N., Andersson Svahn, H., 2012. Droplet microfluidics–a tool for single-cell analysis. Angew Chem. Int. Ed. Engl. 51 (49), 12176–12192.

Lance, S.T., Sukovich, D.J., Stedman, K.M., Abate, A.R., 2016. Peering below the diffraction limit: robust and specific sorting of viruses with flow cytometry. Virol. J. 13 (1), 201.

Lee, M., Lopez-Martinez, M.J., Baraket, A., Zine, N., Esteve, J., Plaza, J.A., Ahmed, N., Elaissari, A., Jaffrezic-Renault, N., Errachid, A., 2015. Combination of PDMS microfilters and micromixers based on flexible thermoplastic films for size sorting and mixing of microparticles. J. Appl. Polym. Sci. 132 (25) (n/a-n/a).

Lim, S.W., Abate, A.R., 2013. Ultrahigh-throughput sorting of microfluidic drops with flow cytometry. Lab Chip 13 (23), 4563–4572.

Liu, J., Sun, G., Wei, S.C., Guo, S., Lin, W.N., Chen, C.H., 2020. Nanoplasmon-enhanced drop-screen for high throughput single-cell nucleocytoplasmic miRNA profiling. Lab Chip 20 (11), 1939–1946.

Liu, Y., Cheng, Y., Zhao, C., Wang, H., Zhao, Y., 2022. Nanomotor-derived porous biomedical particles from droplet microfluidics. Adv. Sci. 9 (4), e2104272.

Liu, Y., Liu, L., Shin, H.D., Chen, R.R., Li, J., Du, G., Chen, J., 2013. Pathway engineering of Bacillus subtilis for microbial production of N-acetylglucosamine. Metab. Eng. 19, 107–115.

Mao, X., Huang, Z., Sun, G., Zhang, H., Lu, W., Liu, Y., Lv, X., Du, G., Li, J., Liu, L., 2021. High level production of diacetylchitobiose deacetylase by refactoring genetic elements and cellular metabolism. Bioresour. Technol. 341, 125836.

Mazutis, L., Gilbert, J., Ung, W.L., Weitz, D.A., Griffiths, A.D., Heyman, J.A., 2013. Single-cell analysis and sorting using droplet-based microfluidics. Nat. Protoc. 8 (5), 870–891.

Nakamura, H., 2011. Application of glucosamine on human disease—Osteoarthritis. Carbohydr. Polym. 84 (2), 835–839.

Ng, E.X., Miller, M.A., Jing, T., Lauffenburger, D.A., Chen, C.H., 2015. Low-volume multiplexed proteolytic activity assay and inhibitor analysis through a pico-injector array. Lab Chip 15 (4), 1153–1159.

Ng, E.X., Sun, G., Wei, S.C., Miller, M.A., DasGupta, R., Lam, P.Y.P., Chen, C.H., 2019. Ultrafast single-cell level enzymatic tumor profiling. Anal. Chem. 91 (2), 1277–1285.

Pan, C.W., Horvath, D.G., Braza, S., Moore, T., Lynch, A., Feit, C., Abbyad, P., 2019. Sorting by interfacial tension (SIFT): label-free selection of live cells based on single-cell metabolism. Lab Chip 19 (8), 1344–1351.

Qiao, Y., Hu, R., Chen, D., Wang, L., Wang, Z., Yu, H., Fu, Y., Li, C., Dong, Z., Weng, Y.X., Du, W., 2022. Fluorescence-activated droplet sorting of PET degrading microorganisms. J. Hazard Mater. 424 (Pt B), 127417.

Qiao, Y., Zhao, X., Zhu, J., Tu, R., Dong, L., Wang, L., Dong, Z., Wang, Q., Du, W., 2017. Fluorescence-activated droplet sorting of lipolytic microorganisms using a compact optical system. Lab Chip 18 (1), 190–196.

Schutz, S.S., Beneyton, T., Baret, J.C., Schneider, T.M., 2019. Rational design of a high-throughput droplet sorter. Lab Chip 19 (13), 2220–2232.

Sitanggang, A.B., Wu, H.S., Wang, S.S., Ho, Y.C., 2010. Effect of pellet size and stimulating factor on the glucosamine production using Aspergillus sp. BCRC 31742. Bioresour. Technol. 101 (10), 3595–3601.

Sivaramakrishnan, M., Kothandan, R., Govindarajan, D.K., Meganathan, Y., Kandaswamy, K., 2020. Active microfluidic systems for cell sorting and separation. Current Opinion in Biomedical Engineering 13, 60–68.

Smith, C.A., Li, X., Mize, T.H., Sharpe, T.D., Graziani, E.I., Abell, C., Huck, W.T., 2013. Sensitive, high throughput detection of proteins in individual, surfactant-stabilized picoliter droplets using nanoelectrospray ionization mass spectrometry. Anal. Chem. 85 (8), 3812–3816.

Sun, L., Bian, F., Wang, Y., Wang, Y., Zhang, X., Zhao, Y., 2020. Bioinspired programmable wettability arrays for droplets manipulation. Proc. Natl. Acad. Sci. U. S. A. 117 (9), 4527–4532.

Tavakoli, H., Zhou, W., Ma, L., Perez, S., Ibarra, A., Xu, F., Zhan, S., Li, X., 2019. Recent advances in microfluidic platforms for single-cell analysis in cancer biology, diagnosis and therapy. Trends Anal. Chem. 117, 13–26.

Watterson, W.J., Tanyeri, M., Watson, A.R., Cham, C.M., Shan, Y., Chang, E.B., Eren, A. M., Tay, S., 2020. Droplet-based high-throughput cultivation for accurate screening of antibiotic resistant gut microbes. Elife 9.

Wen, N., Zhao, Z., Fan, B., Chen, D., Men, D., Wang, J., Chen, J., 2016. Development of droplet microfluidics enabling high-throughput single-cell analysis. Molecules 21 (7).

Wink, K., Mahler, L., Beulig, J.R., Piendl, S.K., Roth, M., Belder, D., 2018. An integrated chip-mass spectrometry and epifluorescence approach for online monitoring of bioactive metabolites from incubated Actinobacteria in picoliter droplets. Anal. Bioanal. Chem. 410 (29), 7679–7687.

Wu, Y., Chen, T., Liu, Y., Tian, R., Lv, X., Li, J., Du, G., Chen, J., Ledesma-Amaro, R., Liu, L., 2020. Design of a programmable biosensor-CRISPRi genetic circuits for dynamic and autonomous dual-control of metabolic flux in Bacillus subtilis. Nucleic Acids Res. 48 (2), 996–1009.

Xi, H.D., Zheng, H., Guo, W., Ganan-Calvo, A.M., Ai, Y., Tsao, C.W., Zhou, J., Li, W., Huang, Y., Nguyen, N.T., Tan, S.H., 2017. Active droplet sorting in microfluidics: a review. Lab Chip 17 (5), 751–771.